Biochemistry

 Volume 38, Number 48 November 30, 1999

Accelerated Publications

Formation of a Pterin Radical in the Reaction of the Heme Domain of Inducible Nitric Oxide Synthase with Oxygen†

Amy R. Hurshman,‡ Carsten Krebs,§ Dale E. Edmondson,|| Boi Hanh Huynh,§ and Michael A. Marletta*,‡,⊥,#

Howard Hughes Medical Institute, Division of Medicinal Chemistry, and Department of Biological Chemistry, University of Michigan, Ann Arbor, Michigan 48109-0606, and Departments of Physics, Biochemistry, and Chemistry, Emory University, Atlanta, Georgia 30322

Received August 30, 1999; Revised Manuscript Received October 6, 1999

ABSTRACT: The heme domain ($iNOS_{heme}$) of inducible nitric oxide synthase (NOS) was expressed in *Escherichia coli* and purified to homogeneity. Rapid freeze−quench (RFQ) EPR was used to monitor the reaction of the reduced $iNOS_{heme}$ with oxygen in the presence and absence of substrate. In these reactions, heme oxidation occurs at a rate of ∼15 s^{-1} at 4 °C. A transient species with a $g = 2.0$ EPR signal is also observed under these conditions. The spectral properties of the $g = 2.0$ signal are those of an anisotropic organic radical with $S = {}^1/_2$. Comparison of the EPR spectra obtained when $iNOS_{heme}$ is reconstituted with N5-^{14}N- and ^{15}N-substituted tetrahydrobiopterin (H_4B) shows a hyperfine interaction with the pterin N5 nitrogen and identifies the radical as the one-electron oxidized form ($H_3B\cdot$) of the bound H_4B. Substitution of D_2O for H_2O reveals the presence of hyperfine-coupled exchangeable protons in the H_4B radical. This radical forms at a rate of 15−20 s^{-1}, with a slower decay rate that varies (0.12−0.7 s^{-1}) depending on the substrate. At 127 ms, $H_3B\cdot$ accumulates to a maximum of 80% of the total $iNOS_{heme}$ concentration in the presence of arginine but only to ∼2.8% in the presence of NHA. Double-mixing RFQ experiments, where NHA is added after the formation of $H_3B\cdot$, show that NHA does not react rapidly with $H_3B\cdot$ and suggest that NHA instead prevents the formation of the H_4B radical. These data constitute the first direct evidence for an NOS-bound $H_3B\cdot$ and are most consistent with a role for H_4B in electron transfer in the NOS reaction.

Nitric oxide synthase (NOS,[1] EC 1.14.13.39) catalyzes the conversion of L-arginine to citrulline and ·NO (*1*−*3*). The overall reaction is a five-electron oxidation, with N^G-hydroxy-L-arginine (NHA) as an intermediate (*4*, *5*), and requires NADPH and O_2 as cosubstrates. Three isoforms of NOS have

† This research was supported by the Howard Hughes Medical Institute and NIH Grants CA 50414 (M.A.M.), GM 29433 (D.E.E.), and GM 47295 (B.H.H.). A.R.H. was supported by NIH Grant T32-GM07767, a Regents' Fellowship from the University of Michigan, and an American Foundation for Pharmaceutical Education Fellowship.

* To whom correspondence should be addressed.
‡ Division of Medicinal Chemistry, University of Michigan.
§ Department of Physics, Emory University.
|| Departments of Biochemistry and Chemistry, Emory University.
⊥ Howard Hughes Medical Institute, University of Michigan.
Department of Biological Chemistry, University of Michigan.

[1] Abbreviations: NOS, nitric oxide synthase; iNOS, inducible NOS; eNOS, endothelial NOS; nNOS, neuronal NOS; $iNOS_{heme}$, heme domain of inducible NOS; IPTG, isopropyl β-D-thiogalactopyranoside; H_4B, (6*R*)-5,6,7,8-tetrahydro-L-biopterin; ^{15}N-H_4B, [5-^{15}N]-(6*R*,*S*)-5,6,7,8-tetrahydro-L-biopterin; HEPES, 4-(2-hydroxyethyl)-1-piperazineethanesulfonic acid; DTT, dithiothreitol; Tris-HCl, tris(hydroxymethyl)-aminomethane hydrochloride; NHA, N^G-hydroxy-L-arginine; ^{15}N-NHA, [^{15}N]-N^G-hydroxy-L-arginine (^{15}N label only at the hydroxylamino nitrogen); HPLC, high-performance liquid chromatography; BSA,

10.1021/bi992026c CCC: $18.00
Published on Web 11/11/1999

been characterized: a particulate, constitutive enzyme from vascular endothelium (eNOS), a soluble, constitutive enzyme from neuronal cells (nNOS), and an inducible enzyme, best characterized from murine macrophages (iNOS) (*6*). All of the isoforms are homodimeric and bind an equivalent each of FAD and FMN (*7*−*9*) as well as iron protoporphyrin IX heme (*10*−*12*) per subunit. Full activity also requires one H_4B per monomer (*9*, *13*, *14*).

The roles of the enzyme-bound heme and H_4B in the reaction mechanism are not fully understood. CO inhibition studies have suggested that the heme is involved in both steps of the NOS reaction (*10*, *15*). Further evidence for the involvement of the heme in NHA oxidation comes from NOS reactions where hydrogen peroxide is substituted for NADPH and O_2 (peroxide-shunt reactions). The products of the peroxide-shunt reactions are consistent with a heme ferric−peroxide nucleophile as an intermediate in the NADPH-dependent oxidation of NHA (*16*, *17*). Since neither peroxide nor iodosobenzene supports the hydroxylation of arginine, the exact function of the heme in this step of the reaction is less clear. Recent results with H_4B-free iNOS have shown that H_4B is absolutely required for the reaction with arginine (*18*). Additionally, the products of NHA oxidation are different in the presence and absence of H_4B, implicating a role for the pterin cofactor in this step as well.

To further elucidate the function of these cofactors in the NOS reaction, we have expressed and purified the heme domain of iNOS. The heme domain of NOS binds both the heme and H_4B cofactors, as well as substrate (*19*−*21*). These properties suggest an intact active site and make $iNOS_{heme}$ a useful tool for mechanistic studies. In particular, it is ideal for examining the formation of intermediates that may form in the NOS reaction, since there is no spectral contribution from the flavins in the reductase domain that might interfere with the observation of any transient species. Furthermore, although the absence of the flavins requires the use of an alternate source of reducing equivalents, such as sodium dithionite, tighter control over the number of electrons delivered to the active site is achieved.

We report here the observation of a novel EPR signal during the reaction of reduced $iNOS_{heme}$ with oxygen. Characterization of this signal suggests that it is due to an NOS-bound trihydropterin radical ($H_3B^{\bullet}$). The possible involvement of this radical in the NOS reaction, particularly in electron transfer, and the implications for NOS catalysis are discussed.

EXPERIMENTAL PROCEDURES

Materials and General Methods. *Escherichia coli* JM109 competent cells were purchased from Promega. Terrific broth (TB) was from Gibco-BRL. Ampicillin and IPTG were from Boehringer-Mannheim. iNOS cDNA in pBluescript II KS was a gift from Dr. Solomon H. Snyder (Johns Hopkins University). The pCWori plasmid (ampicillin resistance, tac-tac promoter) was a gift from Dr. Michael R. Waterman (Vanderbilt University). H_4B and ^{15}N-H_4B (labeled at N5) were purchased from Schircks Laboratories (Jona, Switzerland) and were prepared either in 100 mM HEPES (pH 7.5) containing 100 mM DTT or anaerobically in 100 mM HEPES (pH 7.5) with no DTT. Coomassie Blue R-250 and Bradford protein reagent dye were purchased from Bio-Rad. Reaction vials and silicone/Teflon septa were obtained from Pierce Chemical Co. Centrifugal filtration units (Ultrafree-15 and Ultrafree-0.5, Biomax-30K NMWL membrane) were from Millipore. NHA was purchased either from Alexis Corp. or from Cayman Chemical Co. (Ann Arbor, MI) and was found to contain less than 2% citrulline contamination as analyzed by HPLC. ^{15}N-NHA (labeled only at the hydroxyl-amino nitrogen) was synthesized as previously described (*5*). Sodium dithionite was purchased from Aldrich; solutions (∼4 mg/mL) were prepared anaerobically in 100 mM HEPES (pH 7.5) and were standardized against potassium ferricyanide before use (*22*). All other reagents were purchased from Sigma.

Expression of iNOS Heme Domain. The cloning and expression of $iNOS_{heme}$ will be reported in detail elsewhere. Briefly, the iNOS heme domain expression vector ($pCWiNOS_{heme}$) was constructed by PCR amplification from the iNOS cDNA, addition of appropriate restriction sites, and ligation into the pCW plasmid. This heme domain construct includes amino acids 1−490 of the iNOS sequence and also contains a C-terminal histidine tag (6×His). Optimal expression of $iNOS_{heme}$ was obtained in JM109 cells grown in Terrific broth (47 g/L TB and 4 mL/L glycerol). Expression cultures (1.5 L of TB containing 50 μg/mL ampicillin) were inoculated (1:100) from an overnight culture of JM109-$pCWiNOS_{heme}$ and were grown at 37 °C to an A_{600} of ∼0.5. The cultures were then cooled to 25 °C, induced by the addition of IPTG (0.4 mM final concentration), and harvested by centrifugation (10 min at 15900*g*) 21 h after induction.

Purification of iNOS Heme Domain. Fresh cell pellets from 9 L of culture were resuspended in 200 mL of lysis buffer (50 mM sodium phosphate, pH 8.0, 300 mM NaCl, 10 mM imidazole, 10% glycerol, 10 μg/mL benzamidine, 5 μg/mL leupeptin, and 1 μg/mL each of pepstatin, chymostatin, and antipain) and lysed in a French pressure cell press (SLM-Aminco, Rochester, NY). Supernatant was prepared by centrifugation for 1 h at 40000*g* and was loaded at 1 mL/min on a 10 mL nickel column (Ni-NTA agarose from QIAGEN). All buffers for the nickel column step contained 50 mM sodium phosphate (pH 8.0), 300 mM NaCl, 10% glycerol, and various amounts of imidazole. The column was washed with 150 mL of buffer containing 10 mM imidazole, and then the protein was eluted with a linear gradient of imidazole (10−500 mM) in 125 mL. Fractions containing $iNOS_{heme}$ were red in color and were pooled on the basis of the A_{280}/A_{428} ratio (ratio of peak <1.6). The Ni-column pool was concentrated to less than 5 mL in an Ultrafree-15 device and was applied to a Superdex 200 gel filtration column (HiLoad 26/60 from Amersham Pharmacia Biotech) equilibrated with 20 mM Tris-HCl (pH 8.0), 2 mM imidazole, and 100 mM NaCl. The major peak (eluting at 1 h 40 min at a flow rate of 1.7 mL/min) was $iNOS_{heme}$. The final purification step was anion exchange (Q-HyperD, 10 μm column from Beckman). Buffers for the anion-exchange column contained 20 mM Tris-HCl (pH 8.0), 2 mM imidazole, and various NaCl concentrations. Following loading of the pooled S200 fractions and washing with 100

bovine serum albumin; SDS−PAGE, sodium dodecyl sulfate−polyacrylamide gel electrophoresis; RFQ, rapid freeze−quench; EPR, electron paramagnetic resonance; EDTA, ethylenediamine-*N*,*N*,*N*′,*N*′-tetraacetic acid; NDA, 2,3-naphthalenedicarboxaldehyde.

mM NaCl, the heme domain was eluted with 300 mM NaCl. Fractions containing $iNOS_{heme}$ were stored at −80 °C. Protein concentration (shown as the concentration of $iNOS_{heme}$ monomer) was determined by the Bradford protein assay with BSA as the standard. The purification method described here yields ∼25 mg of $iNOS_{heme}$, with an A_{280}/A_{428} ratio of 1.3−1.35 and judged to be greater than 95% pure by SDS−PAGE with Coomassie staining.

Reconstitution with H_4B and Arginine. Expressed in *E. coli*, $iNOS_{heme}$ contains no bound pterin, and the omission of H_4B in all purification steps results in a pterin-free $iNOS_{heme}$ preparation. Imidazole in the purification buffers increases the stability of $iNOS_{heme}$ prior to reconstitution, and $iNOS_{heme}$ is therefore purified as the imidazole complex (λ_{max} at 428 nm). Unless otherwise specified, all of the experiments described here were carried out with H_4B-bound $iNOS_{heme}$, reconstituted as follows: $iNOS_{heme}$ (50 μM) was incubated with 500 μM H_4B, 5 mM DTT, and 100 mM arginine for 1 h at 4 °C. The spectrum of $iNOS_{heme}$ following this incubation confirmed a complete conversion to high-spin heme (λ_{max} at 396 nm). H_4B-bound $iNOS_{heme}$ was concentrated to 0.3−1 mM and stored at −80 °C with 30% glycerol in aliquots of <300 μL.

Reduction of iNOS Heme Domain. $iNOS_{heme}$ (<300 μL, reconstituted as described above) was desalted immediately prior to use on Sephadex G25M (PD10 prepacked columns from Amersham Pharmacia Biotech) into 100 mM HEPES (pH 7.5). This desalting step removes imidazole, arginine, glycerol, DTT, and any H_4B that is not bound to $iNOS_{heme}$. Depending on the experiment, the buffer contained no substrate, 1 mM arginine, or 1 mM NHA. $iNOS_{heme}$ was concentrated in Ultrafree-0.5 devices to the desired concentration (200−500 μM). A small amount (0.25 equiv of the $iNOS_{heme}$ concentration) of anaerobic H_4B (no DTT) was added to ensure that all of the protein was pterin-bound. The sample was then transferred to an anaerobic cuvette, made anaerobic by 10 cycles of alternate evacuation and purging with purified argon gas, and reduced with sodium dithionite. Reduction of $iNOS_{heme}$ was monitored spectrophotometrically as the decrease in absorbance at 650 nm (ϵ ∼5000 M^{-1} cm^{-1} for ferric $iNOS_{heme}$ and <1000 M^{-1} cm^{-1} for ferrous $iNOS_{heme}$) and the concomitant increase at 558 nm (ϵ ∼9000 M^{-1} cm^{-1} for ferric $iNOS_{heme}$ and ∼13 000 M^{-1} cm^{-1} for ferrous $iNOS_{heme}$). Sodium dithionite was added until the heme was completely and stably reduced; no additional dithionite was added. The reduced heme domain sample was transferred in an anaerobic chamber to the drive syringe of the freeze−quench instrument.

Pterin-Free iNOS Heme Domain. For pterin-free experiments, $iNOS_{heme}$ as purified (imidazole complex, no bound pterin) was concentrated to 0.3−1 mM and stored at −80 °C in aliquots of <300 μL. Immediately prior to use, pterin-free $iNOS_{heme}$ (<300 μL) was desalted to remove the bound imidazole, concentrated, and made anaerobic exactly as described above, with the exception that no H_4B was added to these samples. Unlike H_4B-bound $iNOS_{heme}$, which is mostly high spin in the presence or absence of substrate, pterin-free $iNOS_{heme}$ is a mixture of high- and low-spin forms. The spectrum of pterin-free $iNOS_{heme}$ has absorbance maxima at 420 nm (Soret) and 542 and 578 nm (α/β bands). At long wavelength, in addition to a peak at 650 nm (a ferric high-spin marker), pterin-free $iNOS_{heme}$ has significant absorbance at 730 nm. For these samples, reduction by sodium dithionite was monitored by the bleaching of both the 650 and 730 nm peaks, along with the increase in absorbance at 558 nm. The spectrum of reduced pterin-free $iNOS_{heme}$ is identical to that of the H_4B-bound samples.

Preparation of RFQ Samples. Rapid freeze−quenching was carried out using an Update Instrument unit with a home-built quenching bath as previously described (*23*, *24*). Reduced $iNOS_{heme}$ (200−300 μM) was mixed with oxygenated buffer (100 mM HEPES, pH 7.5, containing no substrate, 1 mM arginine, or 1 mM NHA) in a 2:1 (v/v) ratio. The buffer was oxygenated by 10 cycles of alternative evacuation and purging with oxygen gas and was allowed to equilibrate on ice for >30 min prior to transfer to the RFQ drive syringe. On the basis of the solubility of O_2 at 0 °C (*25*), the concentration of O_2 in this solution was calculated to be ∼2.2 mM. Reactions were carried out at 4 °C and were quenched at various times after mixing (43 ms −40 s) by freezing in isopentane at −140 °C. Samples were then packed into quartz EPR tubes and stored in liquid nitrogen.

Three-Syringe RFQ. Experiments that required double mixing were accomplished by first mixing reduced $iNOS_{heme}$ (450 μM, no substrate) with oxygenated buffer (100 mM HEPES, pH 7.5, no substrate), allowing the reaction to age for 127 ms, and then mixing with buffer containing either 7 mM arginine or 7 mM NHA. The solutions were mixed in a 4:2:1 (v/v/v) ratio of $iNOS_{heme}$/oxygenated buffer/buffer with substrate. The final concentration of substrate after mixing was 1 mM. The reactions were freeze−quenched at various times (25 ms − 40 s) following the second mixing.

RFQ Controls. Controls for each RFQ experiment were carried out as follows. Oxidized control: A 100 μL aliquot was removed from the $iNOS_{heme}$ sample immediately prior to making the sample anaerobic and was diluted with buffer (50 μL of 100 mM HEPES, pH 7.5, with 1 mM appropriate substrate) in the same ratio (2:1 v/v) as the freeze−quenched samples. This solution was then transferred to an EPR tube and frozen in liquid nitrogen. Reduced control: 100 μL of reduced $iNOS_{heme}$ was transferred to an EPR tube in the anaerobic chamber at the same time the rest of the sample was transferred to the RFQ drive syringe. This control was used as the $t = 0$ point in the time courses.

EPR Spectral Acquisition and Kinetic Analysis. EPR spectra were measured using a Bruker ER-200D-SRC spectrometer equipped with an Oxford Instruments ESR 910 continuous-flow cryostat. All spectra were obtained at $T =$ 10 K with a microwave power of 2 mW, a frequency of 9.65 GHz, a modulation amplitude of 1 mT, and a modulation frequency of 100 kHz. Spin quantitations were performed by double integration using a 3 mM Cu-EDTA standard under nonsaturating conditions. Kinetic analysis of heme oxidation was carried out by fitting to a single exponential (A → B, with B being the ferric heme). The $g = 2.0$ data were fit by assuming two sequential irreversible first-order steps for the formation and decay of the radical species (A → B → C, where B is the radical).

Isotope Substitutions. The ^{15}N-H_4B-containing $iNOS_{heme}$ was obtained by incubating pterin-free $iNOS_{heme}$ with ^{15}N-H_4B instead of ^{14}N-H_4B in the reconstitution procedure described above. ^{15}N-H_4B bound to $iNOS_{heme}$ as expected and was able to effect a complete shift to high-spin heme,

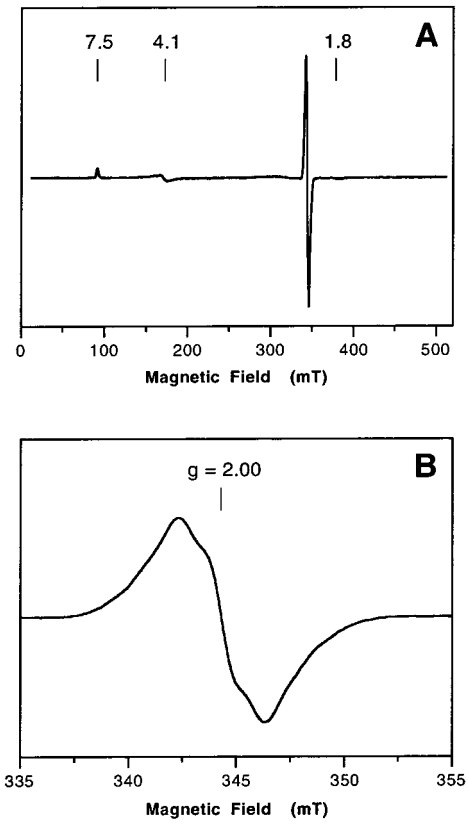

FIGURE 1: EPR spectra of a rapid freeze−quenched sample (127 ms) from the reaction of reduced $iNOS_{heme}$ with oxygen in the presence of arginine. Final concentrations after mixing were 225 μM $iNOS_{heme}$, 730 μM O_2, and 1 mM arginine. (A) Full spectrum, showing the ferric iNOS heme signal (g = 7.5, 4.1, and 1.8) and the g = 2.0 radical. (B) Spectrum of the g = 2.0 region. EPR conditions were as described in Experimental Procedures.

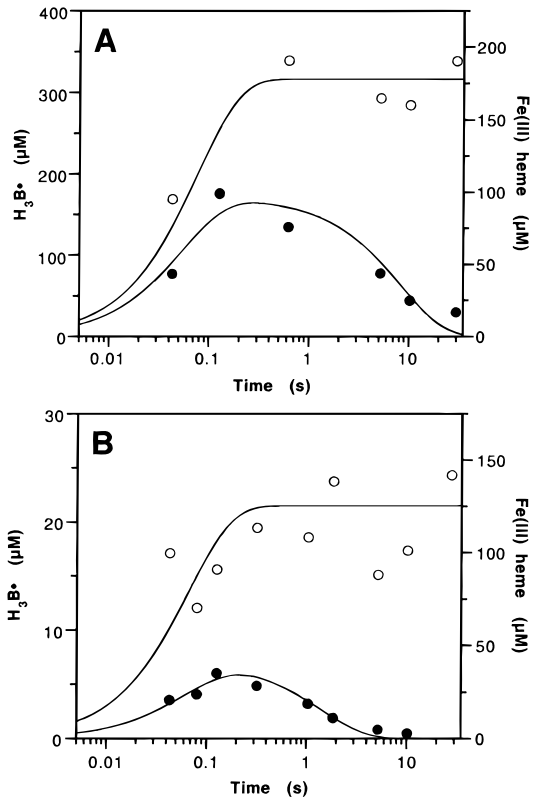

FIGURE 2: Time course of the reaction of reduced $iNOS_{heme}$ with oxygen in the presence of arginine (A, 225 μM $iNOS_{heme}$) or NHA (B, 215 μM $iNOS_{heme}$). The relative amount of radical (●, left axes) at each time point was determined from the peak-to-peak height of the g = 2.0 signal. These numbers were converted to concentrations by double integration of the g = 2.0 signal at 127 ms using Cu-EDTA as the standard. The concentrations of ferric heme (○, right axes) were determined from the peak height of the g = 7.5 signal at each time point relative to that in the oxidized control. The heme concentration in the oxidized control was independently measured by the absorbance of the Soret peak, using an extinction coefficient of 85000 M^{-1} cm^{-1} at 396 nm for substrate-bound $iNOS_{heme}$. The calculated rates from the shown fits are (A) 15 s^{-1} for heme oxidation, 18 s^{-1} for the formation of $H_3B\bullet$, and 0.12 s^{-1} for its decay and (B) 15 s^{-1} for heme oxidation, 15 s^{-1} for the formation of $H_3B\bullet$, and 0.7 s^{-1} for its decay.

as observed with ^{14}N-H_4B. For the D_2O experiments, $iNOS_{heme}$ was desalted and concentrated as described above. The sample was then diluted (5×) in deuterated buffer (100 mM HEPES, 1 mM arginine, pH 7.9, made up in 99.9% D_2O) and concentrated. The final concentration of D_2O was >99.5% following four iterations of dilution/concentration. RFQ was carried out on these samples exactly as described for the ^{14}N-H_4B/H_2O $iNOS_{heme}$.

Quantitation of Amino Acids. Samples retrieved after mixing in the RFQ instrument (not freeze−quenched, t = ∞) were analyzed for product formation. Amino acids were derivatized with NDA and quantified by reverse-phase HPLC as previously described (*17*) with the following modification: Elution conditions were 0−50% solvent B (methanol) in 7 min, followed by a linear increase to 100% solvent B in 2 min, and 100% solvent B for 3 min. Retention times: citrulline, 6.6 min; NHA, 8.7 min; arginine, 9.1 min; phenylalanine (used as an internal standard), 10.2 min.

RESULTS

Observation of a g = 2.0 Signal. Figure 1 shows the EPR spectrum of $iNOS_{heme}$ after reaction with oxygen for 127 ms in the presence of 1 mM arginine. In addition to the expected ferric high-spin heme signal (g = 7.5, 4.1, and 1.8), an additional signal is observed at g = 2.0 (Figure 1A). An expanded spectrum of the g = 2.0 region is shown in Figure 1B. The peak-to-trough line width measures ∼40 G, and some hyperfine structure of the "powder" spectrum is apparent. The saturation properties of this signal ($P_{1/2}$ = 1.8 mW at 10 K) are clearly different from those of the ferric heme signal ($P_{1/2}$ = 22 mW at 10 K) and exhibit a distinct temperature behavior ($P_{1/2}$ increases to 14.5 mW at 80 K; data not shown). As expected for an organic radical, no alterations in line shape of the g = 2.0 signal are observed in the temperature range of 10−80 K.

Time Dependence of the EPR Signal. The amount of radical observed varies with the reaction time, with the maximum intensity observed at 127 ms (Figure 2). Furthermore, the amount of radical formed is also dependent on substrate. In the presence of 1 mM arginine, the concentration of the radical formed at 127 ms is ∼80% of the concentration of $iNOS_{heme}$ monomer (Figure 2A); in the absence of substrate (data not shown) or in the presence of 1 mM NHA (Figure 2B), the maximum concentration is lower, ∼40% and only ∼2.8%, respectively. In all cases, the rate of radical formation is 15−20 s^{-1}. The g = 2.0 signal decays with a $t_{1/2}$ of ∼6 s (k ∼0.12 s^{-1}) in the presence of arginine and ∼1 s (k ∼0.7 s^{-1}) in the presence of NHA. When the radical is formed in the absence of substrate, its decay rate is similar

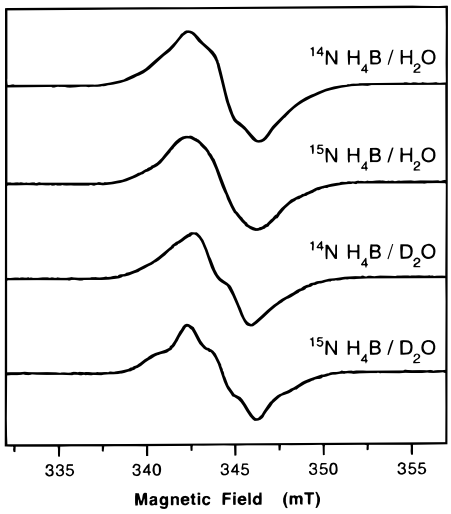

FIGURE 3: Effect of isotope substitutions on the $g = 2.0$ radical signal. The four spectra shown are from samples quenched at 127 ms after mixing of reduced iNOS$_{heme}$ with oxygen in the presence of arginine. Isotope substitutions were effected as described in Experimental Procedures.

to that observed in the arginine sample ($t_{1/2} \sim 6$ s); subsequent addition of either 1 mM arginine or 1 mM NHA does not accelerate the decay of the radical signal (double-mixing experiment; data not shown). Heme oxidation in these experiments occurs simultaneously with radical formation, with a rate of ~ 15 s^{-1} independent of substrate. No other EPR-active species are observed under the reaction conditions used. No $g = 2.0$ signal is observed in similar freeze−quench experiments with pterin-free iNOS$_{heme}$ (1 mM arginine, $t = 127$ ms−5 s). Furthermore, no ferric heme signal is observed in the pterin-free samples, even after 5 s of reaction time.

Isotope Substitutions. Identical experiments were carried out with the following isotope combinations: ^{14}N-H$_4$B/H$_2$O, ^{15}N-H$_4$B/H$_2$O, ^{14}N-H$_4$B/D$_2$O, and ^{15}N-H$_4$B/D$_2$O. The spectra at 127 ms are shown in Figure 3. The spectra obtained in the presence of ^{15}N-H$_4$B differ from those with ^{14}N-H$_4$B in their overall shape and in resolution. Small alterations in spectral properties are also observed on comparison of spectra in D$_2$O with those in H$_2$O. Since these are "powder pattern" anisotropic spectra, the differences in total line width on isotopic substitution are expected to be small. The final isotope substitution we made was with NHA. No differences were observed in EPR spectra obtained with ^{15}N-NHA as compared to those with ^{14}N-NHA (data not shown).

Product Analysis. The identity and stoichiometry (relative to the concentration of the iNOS$_{heme}$ monomer) of the amino acid products from the RFQ reactions with H$_4$B-bound iNOS$_{heme}$ are as follows: 0.78 ± 0.11 NHA ($n = 4$) is formed in the arginine reactions, and 0.63 citrulline ($n = 1$) when NHA is the substrate. Pterin-free iNOS$_{heme}$ does not catalyze NHA formation from arginine in these experiments.

DISCUSSION

In this study, we used rapid freeze−quench EPR to examine the NOS reaction in iNOS$_{heme}$. This technique allows the trapping and subsequent detection of paramagnetic intermediates. In particular, we were interested in testing our proposed mechanism for the oxidation of NHA (*2*). The initial step in this mechanism involves a one-electron oxidation of NHA by the heme ferrous−dioxygen species to form ·NHA. There is no evidence in these experiments for ·NHA. A small amount of a $g = 2.0$ EPR signal is observed upon reaction of NHA-bound, reduced iNOS$_{heme}$ with oxygen. This signal cannot be attributed to ·NHA for two reasons: (1) there is no change in the signal when we substitute ^{15}N-NHA for ^{14}N-NHA, and (2) the same type of radical is formed in the absence of NHA. Our results do not rule out ·NHA as an intermediate in the NOS reaction; they do, however, indicate that if this radical is formed, the decay rate must be faster than the rate of formation.

All of the data presented here are consistent with the assignment of the $g = 2.0$ signal as an NOS-bound pterin radical. Pterin radicals have previously been generated chemically under acidic conditions, either by reaction of reduced pterin with oxidants such as hydrogen peroxide (*26*−*29*) or via the comproportionation reaction of tetrahydro- and dihydropterin (*30*). Both monohydro- and trihydropterin radicals have been described in these reactions, and simulations of the signals are consistent with both species being protonated ($H_2P\cdot^+$ and $H_4P\cdot^+$, respectively), as would be expected at acidic pH (*26*, *28*). A blue, neutral semiquinone ($H_3P\cdot$) has also been observed when 6,6,7,7-tetramethyltetrahydropterin reacts with the corresponding dihydropterin (*30*). The relevance of pterin radicals to catalysis by pterin-containing enzymes is not clear. A trihydropterin radical ($H_3P\cdot/H_4P\cdot^+$) has been suggested as an intermediate in pterin-dependent hydroxylation reactions such as that catalyzed by phenylalanine hydroxylase (PAH) (*31*−*34*). To date, however, no evidence for the formation of a pterin radical intermediate in these enzymes has been reported. A recent paper describes the characterization of a radical species of the molybdopterin cofactor in several bacterial aldehyde dehydrogenases (*35*). This radical is present in the enzymes as isolated and is proposed to be a molybdenum(VI) trihydropterin radical, and the authors suggest that it may be involved in electron transfer from the molybdenum center to one of the iron−sulfur clusters.

The EPR spectral properties of the $g = 2.0$ signal in iNOS$_{heme}$ are those of an anisotropic organic radical. The peak-to-trough line width of 40 G is independent of temperature in the range of 10−80 K. This line width is broader than the well-studied anionic and neutral flavoprotein semiquinones, which exhibit line widths of 16 and 20 G, respectively (*36*). The crystal structures of NOS show that the bound pterin is located in close proximity to the heme (*19*−*21*), and the broad line width observed suggests that this $S = {}^1/_2$ radical may interact magnetically with the $S = {}^5/_2$ heme. Although the different relaxation properties of the $g = 2.0$ (pterin radical) and $g = 7.5$ (ferric iNOS heme) signals indicate that they are not strongly coupled, evidence does exist for a weak magnetic interaction. The measured $P_{1/2}$ (1.8 mW at 10 K) for the $g = 2.0$ signal is significantly greater than that ($\sim 1-10$ μW) of an isolated protein-bound organic radical (*37*) and resembles a situation where the radical relaxation is enhanced by a nearby metal center (*38*). A weak interaction with the nearby heme could have a significant effect on the EPR spectrum and likely accounts for the broad line width of the $g = 2.0$ signal. Another possible explanation for the 40 G line width is the presence of strong hyperfine couplings with protons and/or nitrogens. Further studies are required to elucidate the contributions of

these two mechanisms to the observed line width.

We carried out experiments with various isotope substitutions to further characterize the observed radical. The strongest evidence supporting the identification of the $g = 2.0$ signal as a pterin radical comes from nitrogen substitutions. Substitution of an $I = {}^1/_2$ ^{15}N for the $I = 1$ ^{14}N nucleus at the N5 position of the pterin results in distinct changes in the overall shape and splitting of the EPR signal. These differences are observed both in H_2O and in D_2O, although they appear more pronounced in D_2O. Similar results are obtained when the EPR spectral properties of N5-^{14}N- and ^{15}N-substituted FMN flavodoxin neutral semiquinones are compared (D. E. Edmondson, unpublished observations). This observed effect of the pterin N5 on the radical signal indicates an interaction between this nucleus and the electron spin and suggests that there is significant spin density at N5, as observed in EPR studies on the pterin cation radical (*26, 28*). Exchanging D_2O for H_2O with either nitrogen isotope demonstrates the presence of hyperfine-coupled exchangeable protons, and the smaller magnetic moment of the $I = 1$ D nucleus results in enhanced resolution of the observed EPR spectra. The exchangeable protons are presumably those at the N8 and N5 positions of the pterin. These results are consistent only with a pterin radical.

The potential involvement of a pterin radical in NOS has recently been discussed. The first proposal that $H_3B^{\bullet}$ may function in electron transfer in NOS was based on differences in the spectral decay of the $Fe^{II}O_2$ complex of nNOS in the presence and absence of H_4B (*39*). A second paper (*20*) has compared the structural features of the NOS pterin-binding site to those of other pterin enzymes. The authors propose that the unique hydrogen-bonding interactions of the NOS-bound H_4B may stabilize a pterin radical. They favor a cationic species because of their observation that arginine binds in the pterin binding site of the pterin-free eNOS heme domain crystallized in the presence of *S*-ethylisothiourea. The precise chemical and electronic structure of the $iNOS_{heme}$-bound pterin radical cannot be determined from the anisotropic signals observed in X-band EPR spectra. The observed radical is probably a trihydropterin radical (one-electron oxidized from H_4B), since it is unlikely that a monohydropterin species (oxidized by three electrons) would form under the experimental conditions. Although we represent the radical as $H_3B^{\bullet}$, the relevant enzyme-bound species may be either neutral or cationic.

The time dependence of the EPR spectra shows that heme oxidation ($\sim$15 s^{-1}) occurs in the same time range as pterin radical formation (15−20 s^{-1}). $H_3B^{\bullet}$ is not formed in reactions with pterin-free $iNOS_{heme}$ in the presence of arginine, and heme oxidation is very slow under these conditions (no ferric heme is observed even after 5 s of reaction time). The presence of bound H_4B in NOS is known to influence dimerization (*40*−*42*), heme spin state (*18, 43*) and redox potential (*44*), and affinity for substrate (*45, 46*). Therefore, a similar indirect effect of H_4B on the stability and reactivity of the ferrous heme is not unreasonable. Alternatively, these results may reflect an increased stability of the ferrous−dioxygen complex in the absence of H_4B, consistent with a role for H_4B in electron transfer to the heme. The recently reported NOS structures (*19*−*21*) show the two cofactors in close general proximity, with their relevant atoms (i.e., N5 of the pterin and the iron of the heme) 14 Å apart (T. L. Poulos, personal communication).

The amount of $H_3B^{\bullet}$ observed in these experiments depends on which substrate is present; in the presence of arginine the maximum accumulation of $H_3B^{\bullet}$ is 30-fold greater than that in the presence of NHA. The faster decay rate of the radical in the presence of NHA (0.7 vs 0.12 s^{-1} with arginine) at most would account for a 10% decrease in the maximum amount of radical observed. Two possible explanations for the small accumulation of $H_3B^{\bullet}$ with NHA-bound heme domain are (1) that NHA reacts rapidly with the pterin radical or (2) that the presence of NHA prevents the formation of $H_3B^{\bullet}$. The three-syringe, double-mixing experiment described above shows that the radical once formed does not react with either arginine or NHA. This result argues against a fast reaction of the pterin radical with NHA and suggests that the presence of NHA prevents the one-electron oxidation of H_4B. One way this could occur is if NHA itself reduces the ferrous−dioxygen complex in a single electron-transfer reaction; however, we have no direct evidence for the formation of $^{\bullet}$NHA. We cannot rule out the possibility that NHA is not able to gain access to the active site in this experiment.

Although caution must be used in extrapolating the results obtained here with $iNOS_{heme}$ to the full-length enzyme, characterization of $iNOS_{heme}$ shows that it behaves nearly identically to native iNOS. Purified $iNOS_{heme}$ is dimeric (H_4B-bound or pterin-free, analytical gel filtration on a TosoHaas QC-PAK TSK 300GL column in 100 mM HEPES, pH 7.5, with 200 mM NaCl), and the spectral features of the heme are identical to those of full-length NOS (A. R. Hurshman and M. A. Marletta, unpublished observations). Arginine and NHA bind to $iNOS_{heme}$ with similar affinity as to iNOS and convert the heme completely to the high-spin form. Furthermore, $iNOS_{heme}$ catalyzes the oxidation of both substrates. Together with the EPR data, product formation in the RFQ experiments (NHA from arginine; citrulline from NHA) suggests that $H_3B^{\bullet}$ is formed in the hydroxylation of arginine and that $H_3B^{\bullet}$ formation is not required for the oxidation of NHA. The lack of reactivity of arginine with pterin-free $iNOS_{heme}$ is also consistent with the involvement of H_4B in this step. These observations support a catalytic role for the pterin radical in NOS.

The results reported here can be explained by the model shown in Scheme 1 (*47*). $H_3B^{\bullet}$ is formed in step 1 by reduction of the ferrous−dioxygen ($Fe^{II}O_2$) complex. Subsequent heterolytic cleavage of the ferric−peroxide (Fe^{III}-OOH) species then generates a high-valent iron−oxo complex [$(FeO)^{3+}$], which can hydroxylate arginine as in P450-catalyzed reactions. In step 2, $H_3B^{\bullet}$ does not form because the second electron for Fe^{III}-OOH formation is derived from NHA. This model is consistent with a mechanism that we have previously proposed for the oxidation of NHA (*2*) and for which there is additional support from peroxide-shunt experiments (*16, 17*). The fact that we do not see $^{\bullet}$NHA in the EPR spectra indicates that if this proposed intermediate is formed, it must have a fast decay rate. Since the electron to reduce the $Fe^{II}O_2$ complex derives either from H_4B or from NHA, we also expect to see $H_3B^{\bullet}$ formed in reactions where there is no substrate, as observed. There is no evidence in our EPR spectra for the formation of Fe^{III}-OOH; the only heme species we observe is the oxidized Fe^{III} heme. The Fe^{III}-OOH intermediate once formed can decay in one of

Scheme 1: Model for the Oxidation of Arginine and NHA by NOS

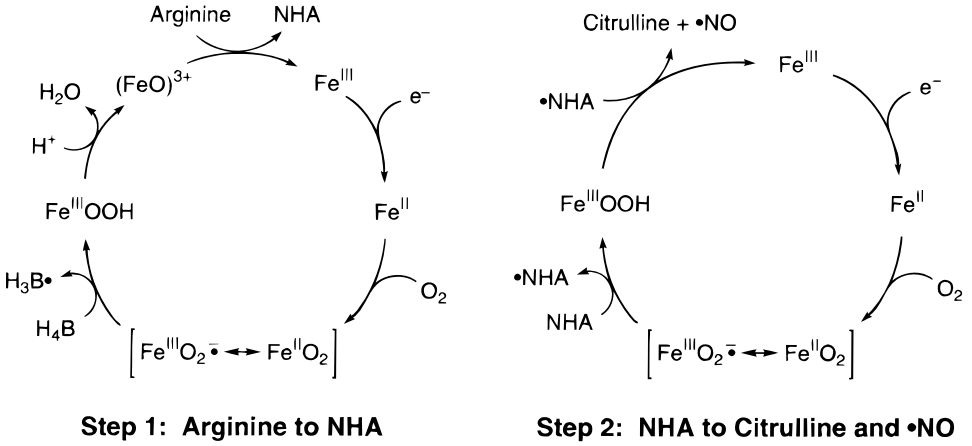

Step 1: Arginine to NHA **Step 2: NHA to Citrulline and •NO**

three ways, depending on the experimental conditions: heterolytic cleavage to the high-valent iron−oxo complex in the hydroxylation of arginine, nucleophilic attack on •NHA to form citrulline and •NO, or release of H_2O_2 in the absence of substrate. Oxidation to the Fe^{III} heme occurs with the same rate as radical formation (15−20 s^{-1}) regardless of which substrate is present. This observation suggests that the decay of Fe^{III}-OOH by any of these three pathways is much faster than 15 s^{-1}.

The simplest model for electron transfer that takes into account the formation of $H_3B\bullet$ is that electrons derived from NADPH proceed through the flavins in the reductase domain to the bound pterin and then finally to the heme. Redox potential differences between arginine and NHA may explain the difference in the source of the second electron for each step. Our ability to observe an apparently stable $H_3B\bullet$ is probably due to the fact that we have used the isolated heme domain and have strictly controlled the number of reducing equivalents in the reaction. In the full-length enzyme, any pterin radical generated during turnover would be rapidly reduced by NADPH-derived electrons from the flavoprotein reductase domain. This role for H_4B in electron transfer in NOS explains the absolute requirement for bound H_4B in the oxidation of arginine (*18*), but it fails to answer two key questions about the NOS mechanism. (1) Why is arginine not a substrate in the peroxide-shunt reaction? If this step is a heme-dependent hydroxylation, hydrogen peroxide is expected to support this reaction, especially since it does support NHA oxidation by NOS (*16, 17*). (2) What is the role of H_4B in the oxidation of NHA? The products of NHA oxidation have been shown to differ in H_4B-bound and H_4B-free iNOS (*18*). The data presented here do not address these questions.

There has been much discussion about the role of H_4B in NOS, particularly concerning the involvement of this cofactor in the hydroxylation of arginine. Recent results, primarily from the crystal structures of NOS, indicate that the role of the pterin in NOS is different from that in the aromatic amino acid hydroxylases. Two recent papers speculate on the involvement of a pterin radical in the NOS reaction, on the basis of the spectral decay of the $Fe^{II}O_2$ complex (*39*) or the structural features of the pterin binding site (*20*). Our results provide the first evidence that a pterin radical is formed in NOS and are most consistent with H_4B being involved in electron transfer in NOS. Specifically, H_4B would reduce the heme ferrous−dioxygen complex, and the resulting $H_3B\bullet$ would subsequently be reduced by the NOS flavins. This is an unprecedented chemical role for this cofactor.

ACKNOWLEDGMENT

We thank Sylvia Zhao for providing some of the protein used in these experiments and Robert A. Pufahl for synthesizing ^{15}N-labeled NHA. We also thank Melissa J. Clague and Kristin M. Rusche for their mechanistic insights and the members of the Marletta laboratory for helpful suggestions.

REFERENCES

1. Marletta, M. A., Hurshman, A. R., and Rusche, K. M. (1998) *Curr. Opin. Chem. Biol. 2*, 656−663.
2. Marletta, M. A. (1993) *J. Biol. Chem. 268*, 12231−12234.
3. Nathan, C. (1992) *FASEB J. 6*, 3051−3064.
4. Stuehr, D. J., Kwon, N. S., Nathan, C. F., Griffith, O. W., Feldman, P. L., and Wiseman, J. (1991) *J. Biol. Chem. 266*, 6259−6263.
5. Pufahl, R. A., Nanjappan, P. G., Woodard, R. W., and Marletta, M. A. (1992) *Biochemistry 31*, 6822−6828.
6. Marletta, M. A. (1994) *Cell 78*, 927−930.
7. Hevel, J. M., White, K. A., and Marletta, M. A. (1991) *J. Biol. Chem. 266*, 22789−22791.
8. Stuehr, D. J., Cho, H. J., Kwon, N. S., Weise, M. F., and Nathan, C. F. (1991) *Proc. Natl. Acad. Sci. U.S.A. 88*, 7773−7777.
9. Mayer, B., John, M., Heinzel, B., Werner, E. R., Wachter, H., Schultz, G., and Böhme, E. (1991) *FEBS Lett. 288*, 187−191.
10. White, K. A., and Marletta, M. A. (1992) *Biochemistry 31*, 6627−6631.
11. Stuehr, D. J., and Ikeda-Saito, M. (1992) *J. Biol. Chem. 267*, 20547−20550.
12. McMillan, K., Bredt, D. S., Hirsch, D. J., Snyder, S. H., Clark, J. E., and Masters, B. S. (1992) *Proc. Natl. Acad. Sci. U.S.A. 89*, 11141−11145.
13. Hevel, J. M., and Marletta, M. A. (1992) *Biochemistry 31*, 7160−7165.
14. Schmidt, H. H. H. W., Smith, R. M., Nakane, M., and Murad, F. (1992) *Biochemistry 31*, 3243−3255.
15. Pufahl, R. A., and Marletta, M. A. (1993) *Biochem. Biophys. Res. Commun. 193*, 963−970.
16. Pufahl, R. A., Wishnok, J. S., and Marletta, M. A. (1995) *Biochemistry 34*, 1930−1941.
17. Clague, M. J., Wishnok, J. S., and Marletta, M. A. (1997) *Biochemistry 36*, 14465−14473.
18. Rusche, K. M., Spiering, M. M., and Marletta, M. A. (1998) *Biochemistry 37*, 15503−15512.

19. Crane, B. R., Arvai, A. S., Ghosh, D. K., Wu, C., Getzoff, E. D., Stuehr, D. J., and Tainer, J. A. (1998) *Science 279*, 2121−2126.
20. Raman, C. S., Li, H., Martasek, P., Kral, V., Masters, B. S., and Poulos, T. L. (1998) *Cell 95*, 939−950.
21. Fischmann, T. O., Hruza, A., Niu, X. D., Fossetta, J. D., Lunn, C. A., Dolphin, E., Prongay, A. J., Reichert, P., Lundell, D. J., Narula, S. K., and Weber, P. C. (1999) *Nat. Struct. Biol. 6*, 233−242.
22. Di Iorio, E. E. (1981) *Methods Enzymol. 76*, 57−72.
23. Ravi, N., Bollinger, J. M., Jr., Huynh, B. H., Edmondson, D. E., and Stubbe, J. (1994) *J. Am. Chem. Soc. 116*, 8007−8014.
24. Ballou, D. P. (1978) *Methods Enzymol. 54*, 85−93.
25. Battino, R. (1981) in *IUPAC Solubility Data Series*, Permagon Press, Oxford, U.K.
26. Ehrenberg, A., Hemmerich, P., Müller, F., Okada, T., and Viscontini, M. (1967) *Helv. Chim. Acta 50*, 411−416.
27. Bobst, A. (1967) *Helv. Chim. Acta 50*, 2222−2225.
28. Bobst, A. (1968) *Helv. Chim. Acta 51*, 607−613.
29. Funahashi, Y., Kohzuma, T., Odani, A., and Yamauchi, O. (1994) *Chem. Lett.*, 385−388.
30. Eberlein, G., Bruice, T. C., Lazarus, R. A., Henrie, R., and Benkovic, S. J. (1984) *J. Am. Chem. Soc. 106*, 7916−7924.
31. Viscontini, M., Leidner, H., Mattern, G., and Okada, T. (1966) *Helv. Chim. Acta 49*, 1911−1915.
32. Ehrenberg, A., Hemmerich, P., Muller, F., and Pfleiderer, W. (1970) *Eur. J. Biochem. 16*, 584−591.
33. Kappock, T. J., and Caradonna, J. P. (1996) *Chem. Rev. 96*, 2659−2756.
34. Francisco, W. A., Tian, G., Fitzpatrick, P. F., and Klinman, J. P. (1998) *J. Am. Chem. Soc. 120*, 4057−4062.
35. Luykx, D. M., Duine, J. A., and de Vries, S. (1998) *Biochemistry 37*, 11366−11375.
36. Palmer, G., Müller, F., and Massey, V. (1971) in *Flavins and Flavoproteins* (Kamin, H., Ed.) pp 123−126, University Press, Baltimore, MD.
37. Hirsh, D. J., Beck, W. F., Innes, J. B., and Brudvig, G. W. (1992) *Biochemistry 31*, 532−541.
38. Szalai, V. A., Kuhne, H., Lakshmi, K. V., and Brudvig, G. W. (1998) *Biochemistry 37*, 13594−13603.
39. Bec, N., Gorren, A. C., Voelker, C., Mayer, B., and Lange, R. (1998) *J. Biol. Chem. 273*, 13502−13508.
40. Baek, K. J., Thiel, B. A., Lucas, S., and Stuehr, D. J. (1993) *J. Biol. Chem. 268*, 21120−21129.
41. Abu-Soud, H. M., Loftus, M., and Stuehr, D. J. (1995) *Biochemistry 34*, 11167−11175.
42. Klatt, P., Schmidt, K., Lehner, D., Glatter, O., Bachinger, H. P., and Mayer, B. (1995) *EMBO J. 14*, 3687−3695.
43. Rodriguez-Crespo, I., Gerber, N. C., and Ortiz de Montellano, P. R. (1996) *J. Biol. Chem. 271*, 11462−11467.
44. Presta, A., Weber-Main, A. M., Stankovich, M. T., and Stuehr, D. J. (1998) *J. Am. Chem. Soc. 120*, 9460−9465.
45. Klatt, P., Schmid, M., Leopold, E., Schmidt, K., Werner, E. R., and Mayer, B. (1994) *J. Biol. Chem. 269*, 13861−13866.
46. White, K. A. (1994) Doctoral Thesis, The University of Michigan, Ann Arbor, MI.
47. Ludwig, M. L., and Marletta, M. A. (1999) *Structure 7*, R73−R79.

BI992026C